Selectivity of Metal-modified HZSM-5 to Nitrogen-Containing Compounds in Two-step Hydrothermal Liquefaction Products of Nitrogen-rich Tobacco Stem

Jing Bai[1,3], Lefei Li[1], Hao Li[2], Pan Li[1,3], Chun Chang[2,3]

Abstract

The main objective of this research was to investigate the selectivity of HZSM-5 zeolite modified by Zn, Cu, and Cr metals to nitrogen-containing compounds (NCCs) in two-step hydrothermal liquefaction (HTL) products of nitrogen-rich tobacco stem (TS). Using GC-MS, XPS, FT-IR, GC, and SEM, the probable reaction process was analyzed for the reaction products. When HZSM-5 was used for catalytic liquefaction, the bio-oil yield was the highest, and the bio-oil contained the highest concentration of NCCs, which reached 64.13%. The modified HZSM-5 did not stimulate the NCCs in bio-oil as effectively as the unmodified HZSM-5. However, metal-modified HZSM-5 was helpful in the production of nicotine in bio-oil, with Cu/HZSM-5 exhibiting the highest selectivity. Cr/HZSM-5 was highly selective for pyrrole; following the catalytic process, the relative amount of pyrrole in bio-oil reached 4.19%. After the introduction of HZSM-5, the coking rate of the reaction products rose regardless of whether they were modified with a single metal, two metals, or three metals. This work provides an improved understanding of the manufacture of NCCs from TS by two-step HTL, as well as modified HZSM-5 for the synthesis of nicotine, pyridine, pyrrole, and pyrazine.

Introduction

Environmental issues and global warming are becoming more prominent due to the widespread use of fossil fuels, and the creation and usage of alternative new energy have steadily emerged as a major trend in societal development (Zhuang et al., 2022). Recently, biomass energy has attracted the attention of many scholars due to its large reserves and rich content (Khanmohammadi et al., 2016). Tobacco, as one of the biomass sources, generates a large amount of waste each year (Banozic et al., 2020). In China, millions of tons of tobacco are produced every year, and many tobacco wastes exist. The traditional burning and utilization method not only has a very low utilization rate but also extremely pollutes the environment (Guo et al., 2021). Therefore, a reasonable method is urgently needed to maximize tobacco waste. Tobacco stem (TS) is the thick and hard vein of tobacco, and it contains about 25%–30% of leaf weight (Gao et al., 2022). The majority of TS is discarded as tobacco waste. Therefore, TS has representative significance in the study of tobacco waste.

Hydrothermal liquefaction (HTL), a sort of thermochemical conversion, is an excellent way to utilize biomass energy because of its low energy consumption and convenient industrialization (Ponnusamy et al., 2020). At present, HTL has two main directions: one is to use bio-oil as biofuel to increase the heat value of bio-oil via reducing the content of N, O, and S in bio-oil; the other is to

Correspondence.   Chun Chang, School of Chemical Engineering, Zhengzhou University, Zhengzhou 450001, China. E-mail address: chunchang@zzu.edu.cn Telephone: +86-371-67781801.

Author Affiliation.
[1] School of Mechanical and Power Engineering, Zhengzhou University, Zhengzhou 450001, China
[2] School of Chemical Engineering, Zhengzhou University, Zhengzhou 450001, China
[3] Henan Center for Outstanding Overseas Scientists, Zhengzhou University, Zhengzhou 450001, China

increase the content of high-value compounds in bio-oil. To increase the content of high-value compounds in HTL products, we often need to add catalysts to increase the yield of some compounds in bio-oil. Zheng et al., (2022) found that NH_3 baking pretreatment of biomass can promote the generation of pyrrole and pyrazine in pyrolysis products, and they pointed out that biomass contains many oxygen-containing functional groups, which can be easily ammonified to form NCCs. Therefore, it has good prospect to produce high value-added NCCs through reasonable regulation of the reaction process. A previous study showed that after adding urea to TS for two-step HTL, the relative content of NCCs in bio-oil can reach 57.34% (Li et al., 2022). The components of NCCs such as nicotine, pyridine, pyrrole, and pyrazine have numerous industrial applications. However, if we want to apply these high-value NCCs in practical production, we need to optimize and improve the experimental process.

Compared with one-step HTL, two-step HTL has its own unique advantages in the preparation of NCCs. Kang et al. (2001) found that two-step HTL is more conducive to protein decomposition into amino acids at about 200 °C than one-step HTL. Li et al. (2022) also found that two-step HTL is more conducive to the formation of NCCs in bio-oil than one-step HTL.

The use of traditional homogeneous catalysts, such as alkali catalysts (e.g., Na_2CO_3, K_2CO_3, KOH, and NAOH) and acid catalysts (HCL and H_2SO_4) can cause serious corrosion to equipment and are difficult to recover (Cheng & Rabnawaz, 2018). Heterogeneous catalysts, such as zeolite, are not only easy to recover but also environmentally friendly, in line with the concept of carbon neutrality, so the use of zeolite catalysts may be promising (Ong et al., 2019). In many heterogeneous catalysts, HZSM-5 is widely used. In the catalytic reaction, HZSM-5 mainly relies on the catalytic action of Bronsted acid and Lewis acid (Yuan et al., 2019). The functions of Lewis acid and Bronsted acid are decarbonylation, decarboxylation, hydrodeoxygenation, cracking, hydrogenation, and hydrocracking reactions. These reactions support the reaction of HZSM-5 to convert oxygenated compounds into hydrocarbons. After metal modification, the internal acid sites of Lewis acid and Bronsted acid of zeolite will change, which play certain selectivity to some compounds in the product. Cheng et al. found that HZSM-5 modified by Zn is beneficial for the aromatization of the compounds in bio-oil after catalytic liquefaction, and co-modification with Zn and Co can reduce the coking rate in the reaction products (Cheng et al., 2018). According to Li et al., (2017), after modifying HZSM-5 with Fe, Co, and Cu, the gas phase yield of catalytic pyrolysis reaction products increases, and the modified HZSM-5 zeolite can also enhance the aromatization of products in bio-oil.

Zeolite also has its disadvantages in the process of catalytic liquefaction. In the process of optimizing bio-oil, as a result of zeolite's rich pore structure, it may absorb some volatile substances, which will increase the quality of the catalyst and reduce the quality of bio-oil (Feng et al.). Despite many studies on the preparation of high-value compounds from metal-modified catalytic bio-oil, work on the promotion of NCCs by metal modification is few. Zhang et al., (2019) found that the Cr/HZSM-5 catalyst improves the selectivity of NCCs (such as acetonitrile, pyridine, and pyrrole) during catalytic pyrolysis of corncob in an ammonia atmosphere. Wu et al., (2020) found that NCCs are selectively treated with Zn-modified HZSM-5, and the bio-oil yield increases. Huang et al.(Z. G. Huang et al., 2022) found that the yield of NCC nitriles significantly increases in the co-pyrolysis experiment of chlorella and urea with the addition of HZSM-5. The addition of HZSM-5 may promote the Maillard reaction to generate five- and six-membered cyclic NCCs. Yao et al., (2015) used zeolite as a catalyst to catalyze the preparation of indole under ammonia atmosphere and found that furfural can react with ammonia on the HZSM-5 catalyst to generate nitrogen-containing heterocyclic compounds, and phenolic compounds can generate various aromatic amines under ammonia atmosphere. The method of preparing high-value NCCs by catalytic liquefaction of metal-modified HZSM-5 zeolite still has remarkable potential.

In addition to NCCs in bio-oil, nitrogen-rich biochar is widely used in industrial production, and nitrogen-doped carbon is widely used in adsorbent, catalyst carrier, and energy conversion (Xu et al., 2017). Wang et al. (2015) synthesized an unusual sheet of activated carbon from catkins and used it as a high-performance supercapacitor. Ren et al. (2014) also developed a 3D nitrogen-doped carbonaceous aerogel made of sugar and polypyrrole, which has excellent specific capacitance.

In this research, we focused on the preparation of high-value NCCs. By adding nitrogen source urea, we discussed the influence of catalysts on the NCCs in the two-step HTL products of HZSM-5 after metal Zn, Cu, and Cr impregnation and modification. Zeolite was characterized and analyzed by XRD, BET, and SEM. Reaction products were analyzed via GC-MS, XPS, FT-IR, and SEM. According to the composition of NCCs in the bio-oil produced by different metal loads, the evolution mechanism of nitrogen that may occur in the HTL process was summarized, which provides some insights into the preparation of high-value NCCs from TS.

2. Materials and methods

2.1. Raw materials

The raw material used in this experiment was TS from Pingdingshan, Henan Province. TS was ground into powder and

stored in a cool, dry place. Urea (analytical reagent, AR) was purchased from Tianjin Yongda Chemical Reagent Co., Ltd., configured with 2 wt% urea reagents, and stored in a cool and dry place.

According to the national standard GB/T 28,731-2012 of the People's Republic of China (PRC) (GB/T: Chinese abbreviation for China Recommended National Standard), the TS samples were analyzed in a close range. The elemental composition of TS was analyzed by an organic element analyzer (Elementar Vario El III) according to the People's Republic of China national standard GB/T 28,731e2012 industrial analysis. Table 1 lists the approximate and elemental analyses.

2.2. Catalysts and characterizations

HZSM-5 zeolite (silicon aluminum ratio 30, particle size 1 mm) was purchased from Dalian Zhuoran Environmental Protection Technology Co., Ltd. and calcined in a muffle furnace at 550 °C for 4 h before modification. The metal-modified catalysts with different metal loadings were prepared via solution immersion. Zinc nitrate ($Zn(NO_3)_2·6H_2O$, AR), cupric nitrate ($Cu(NO_3)_2·6H_2O$, AR), and chromic nitrate ($Cr(NO_3)_3·9H_2O$, AR) were purchased from Rhawn. The required amount of nitrate was dissolved in water (100 mL) and mixed with HZSM-5 (5 g). The mixture was stirred at 25 °C for 4 h and then dried in an oven at 105 °C for 24 h. Finally, these catalysts were calcined in a muffle furnace at 550 °C for 4 h and carefully stored for future use. The HZSM-5 zeolites prepared by the test were HZSM-5, 10% Zn/HZSM-5, 10% Cu/HZSM-5, 10% Cr/HZSM-5, 5% Zn/5% Cu/HZSM-5, 5% Zn/5% Cr/HZSM-5, 5% Cu/5% Cr/HZSM-5, and 3.33% Zn/3.33% Cu/3.33% Cr/HZSM-5.

The crystal phase characteristics of the catalyst were analyzed by X-ray diffraction (XRD) of the X'Pert PRO X-ray diffractometer of PANalytical Company in the Netherlands. The analyzed parameters were set as follows: 40 kV voltage, 40 mA current, copper as anode target, scanning step length of 0.0167°, scanning speed of 5°/min, and scanning range of 10°–80°.

The specific pore volume, surface area, and average pore diameter of the catalyst were analyzed by using BK100-01 automatic specific surface area and pore diameter analyzer of Beijing Jingwei Gaobo Technology Co., Ltd. The catalyst was degassed in vacuum at 300 °C for 5 h, and the samples were analyzed in 77 K liquid nitrogen environment by nitrogen isothermal adsorption and desorption.

The surface characteristics and morphology of the HZSM-5 catalyst were analyzed with a desktop scanning electron microscope (Czech TESCAN MIRA LMS), with a magnification of 5000 times.

2.3. Experimental unit and procedure

Figure1 shows the experimental device used in this experiment. The reaction kettle used in this experiment was an MS series micro autoclave from Anhui Kemi Machinery Technology Co., Ltd. The experiment was carried out in a 100 mL reactor system.

Before each experiment, 4 g of TS and 1 g of HZSM-5 zeolite were weighed, and 60 mL of urea solution with concentration of 2% was weighed and poured into the reactor. Before the reaction, the reactor was purged with N_2 to replace all the air. The reaction conditions were as follows: 200 °C for 15 min, 300 °C for 15 min, and initial pressure of 6 MPa. After the reaction, the reactor was washed with C_3H_6O (acetone) and CH_2Cl_2 (dichloromethane) until all residues in the reactor flowed out, and the flushing solution was clarified. A funnel was used to separate the solid and liquid in the washings. The separated solid biochar was baked in an oven at 105 °C for 24 h, weighed, and collected. The liquid was poured into the separating funnel and then left for layering. The lower oil phase was gleaned and rotated in a rotary evaporator at 65 °C. The oil phase after rotary evaporation was dissolved and collected with C_3H_6O. Each test was repeated three times. In the experiment, the reaction without HZSM-5 zeolite was called "Blank."

2.4. Product analysis and data processing

The bio-oils were analyzed via GC-MS (GC-8860/MS-5977 A, Agilent) on a HP-5MS (30 m×0.25 m×0.25 μm) column. When helium was used, the carrier gas split ratio was 1:50 and the injector temperature was 290 ℃. The GC-measured temperature was maintained at 40 ℃ for 5 min, heated to 280 ℃ at a rate of 5 ℃/min, and maintained at 280 ℃ for 5 min. For MS operating conditions, the MS conditions were as follows: MS interface temperature of 290 ℃, scan range of 30–500 (m/z), and solvent delay time of 2 min.

Coke was tested by using an X-ray photoelectron spectrometer (KRATOS, UltraDLD, the UK). Among them, the vacuum degree of the analysis chamber was 9.8×10−10 Torr, and the excitation source was Al ka ray (hv=1486.6 eV). The full spectrum acquisition voltage was 15 kV, the flame current was 5 mA, and the test passing energy was 160 Ev. The fine spectral voltage was 15 kV, the flame current was 10 mA, and the test passing energy was 40 eV.

Qualitative measurement of biochar was carried out by Fourier transform infrared spectroscopy (Perkin Elmer FT-IR spectrometer) in the spectral range of 400–4000 cm^{-1}. The instrument used in SEM was Czech TESCAN MIRALMS, and the sample pictures were magnified 2000 times. As a result of the weak conductivity of the dry sample, it was metal-sprayed before analysis. Noncondensing gases were analyzed by GC (GC-14C, Shimadzu Corporation). Standard gas control procedures were first used to identify gas types, and external standards were used to quantify the main components of gas products (CO, CO_2, H_2, and CH_4).

The ratio of the weight of residual biochar after drying to the weight of TS before the reaction was used to calculate the biochar yield. The yield of bio-oil was calculated by the ratio of the weight of residual bio-oil collected after spin steaming to the weight of TS before the reaction. The rest was the yield of gas and loss. The yields were determined as shown in Equations (1)–(3):

Table 1. Approximate and elemental analyses of TS samples.

	Element analysis /wt (%)					Approximate analysis /wt (%)			
	C_{ad}	H_{ad}	O_{ad}	N_{ad}	S_{ad}		M_{ad}	A_{ad}	V_{ad}	FC_{ad}
TS	37.57	4.29	54.63	2.28	1.23		17.58	11.11	18.12	52.92

Table 2. Texture characteristics of metal-modified HZSM-5 catalyst.

Catalyst	Surface area (m²/g)	Pore size (nm)	Total pore volume
	BET	Average	(cm³/g)
HZSM-5	335.190	3.691	0.287
Zn/HZSM-5	293.450	3.597	0.249
Cu/HZSM-5	271.258	3.628	0.228
Cr/HZSM-5	289.212	3.626	0.243
Zn/Cu/HZSM-5	298.091	3.402	0.236
Zn/Cr/HZSM-5	290.375	3.494	0.233
Cu/Cr/HZSM-5	281.730	3.417	0.228
Zn/Cu/Cr/HZSM-5	283.103	3.296	0.218
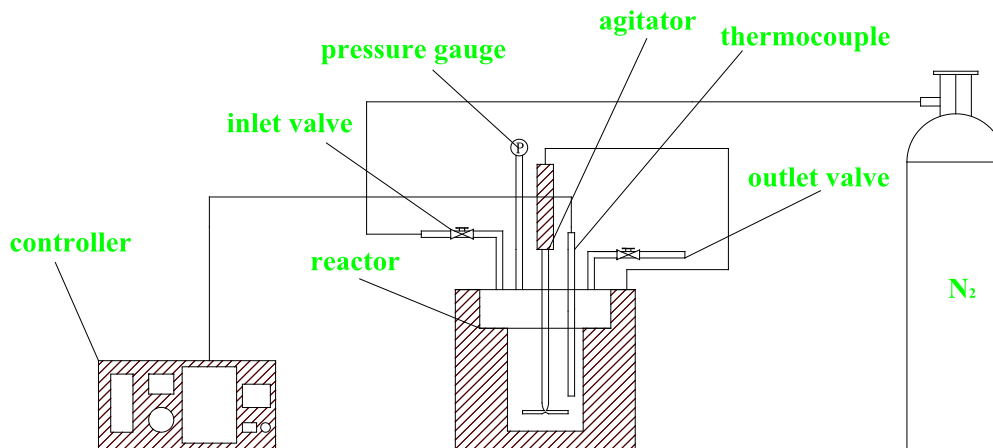
Figure 1. Laboratory-scale hydrothermal liquefaction test device diagram of TS
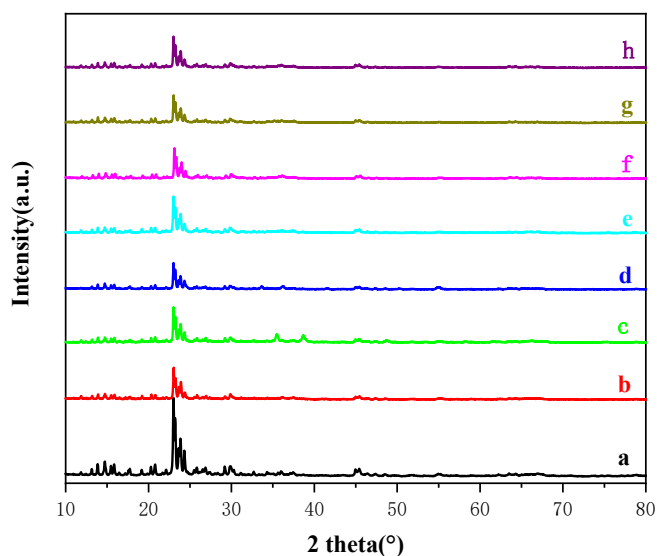
Figure 2. Patterns of XRD characterization for the catalysts. a: HZSM-5, b: Zn/HZSM-5, c: Cu/HZSM-5, d: Cr/HZSM-5, e: Zn/Cu/HZSM-5, f: Zn/Cr/HZSM-5, g: Cu/Cr/HZSM-5, and h: Zn/Cu/Cr/HZSM-5.

$$Y_{biochar} = \frac{m_{biochar}}{M} \qquad (1)$$

$$Y_{bio-oil} = \frac{m_{bio-oil}}{M} \qquad (2)$$

$$Y_{gas\ and\ loss} = \frac{M - m_{biochar} - m_{bio-oil}}{M} \qquad (3)$$

where $Y_{biochar}$, $Y_{bio-oil}$, and $Y_{gas\ and\ loss}$ express the ratios of biochar, bio-oil, and gas and loss, respectively. $m_{biochar}$ and $m_{bio-oil}$ express the ratios of biochar and bio-oil, respectively. M is the weight of biomass.

3. Results and discussion

3.1. Catalyst characterization

By analyzing the BET of zeolite catalyst, we can determine the loading of metal on zeolite after modification. Table 2 lists the basic characteristics of HZSM-5 and metal-modified HZSM-5. Table 2 shows that the specific surface area, pore diameter, and pore volume of HZSM-5 impregnated with Zn, Cu, and Cr were reduced compared with those of HZSM-5. The pores of HZSM-5 modified with Zn, Cu, and Cr were filled with ZnO, CuO, and Cr_2O_3 particles, which may also be caused via the deposition of these particles outside of HZSM-5(Cheng et al., 2017; Li et al., 2017; Zhang et al., 2019).

Figure 2 shows the XRD spectrum of the HZSM-5 zeolite after metal loading modification. In the XRD spectrum of the metal-modified HZSM-5 zeolite catalyst, diffraction peaks corresponding to the structure of the unmodified HZSM-5 zeolite were observed at 7.9°, 8.8°, 23.0°, 23.2°, 23.6°, 23.9°, and 24.4° (Khoshbin & Haghighi, 2013). These peaks showed that the crystal line skeleton of HZSM-5 remained unchanged, and HZSM-5 was not damaged via metal modification after loading modification of Zn, Cu, and Cr. Fig. 3 shows the SEM characterization of HZSM-5. The load of metal-modified HZSM-5 was relatively uniform, which also verified the XRD analysis in Figure 2.

3.2. Effect of catalysts on product yields

The basic characteristics of HZSM-5 modified by different metals were identified by analyzing the yield of catalytic products of various catalysts. Fig. 4 shows the influence of Zn, Cu, and Cr metal-modified HZSM-5 on the content of HTL products of TS in the urea environment.

As shown in Figure 4, after adding HZSM-5, the bio-oil yield increased to 14.5%, which may be because the role of Lewis acid and Bronsted acid promotes the decomposition of macromolecular substances in TS (Zhao et al., 2015) and effectively promotes the conversion reaction in biomass liquefaction, leading to an increase in the content of bio-oil. However, the HZSM-5 zeolite modified by adding single metal Zn, Cu, and Cr had no obvious influence on the content of bio-oil, and the yields were 12.5%, 10.5%, and 13.75%, respectively. Zn and Cu even exerted inhibition effects. ZnO and CuO occupied part of the acidic sites of HZSM-5, leading to incomplete reaction of two-step HTL. Compared with the single metal-modified catalyst, the bimetallic-modified catalysts

Zn/Cu/HZSM-5, Zn/Cr/HZSM-5, and Cu/Cr/HZSM-5 still had little effect on the oil yields, which were 12.5%, 11%, and 13.75%, respectively. However, the catalytic effect of the HZSM-5 zeolite modified by Zn and Cu was more obvious than that of the HZSM-5 zeolite modified by Cu alone. In the case of joint modification, Zn may play a more dominant role in the competitive acid sites. The HZSM-5 zeolite co-modified by Zn and Cr significantly reduced the bio-oil yield of the reaction product, which may be due to the vicious competition of acid sites caused via the mixing of two metals. However, this vicious competition may only occur between Zn and Cr, and the HZSM-5 zeolite modified by Cu and Cr had no impact on the inhibition of the bio-oil yield. For tri metal-modified HZSM-5, no obvious vicious competition of acid sites was found among the three metals. Compared with single metal Cr, the bio-oil production rate did not decrease. Regardless of bimetal or tri metal, in the absence of the vicious competition of metals, dominant metals often dominate the bio-oil production rate. From the perspective of biochar generation, whether HZSM-5 is unmodified or metal-modified, its coking rate is higher than that of HZSM-5 without zeolite, mainly because HZSM-5 is more acidic, which can easily lead to serious coking in the reaction process (Liu et al., 2004). The coking rate of the HZSM-5 zeolite after metal modification decreased because the metal modification changed the total acid amount of Lewis acid and Bronsted acid, thereby changing the total acidity of HZSM-5, so the coking rate decreased. In general, the HZSM-5 zeolite had little effect on the content of bio-oil, but it could significantly boost the production of biochar.

3.3. Effect of catalysts on the chemical compositions of bio-crude

The analysis of the relative content changes of various chemicals in bio-oil via GC-MS can help understand the possible reactions of TS in two-step HTL and elucidate the selectivity of the HZSM-5 zeolite modified by different metals to NCCs. Figs. 5 and 6 show the effect of metal-modified HZSM-5 zeolite on the relative content of the main chemical components in bio-oil of TS after two-step HTL in urea environment.

Figure. 5 and 6 show that the main components of bio-oil were NCCs, ketones, and phenols. NCCs in bio-oil mainly included nicotine, pyridine, pyrrole, pyrazine, and quinoline. After adding zeolite, the total categories of NCCs increased, including the production of piperidine, piperazine, indole, imidazole, pyrimidine, indole, and pyrazole. However, the relative content was small. Each group of experiments for HTL was conducted in a 2% urea environment, which was accompanied with a large number of N elements, with NCCs accounting for a major part in bio-oil. When the HZSM-5 catalyst was not added, the relative content of NCCs in the bio-oil could reach 57.34%. When the HZSM-5 catalyst was added, the relative content of NCCs could reach 64.13%. Thus, the HZSM-5 zeolite promoted the generation of NCCs (Pan et al., 2022). HZSM-5 promoted the Maillard reaction to form five-

HZSM-5

Zn/HZSM-5

Cu/HZSM-5

Cr/HZSM-5

Zn/Cu/HZSM-5

Zn/Cr/HZSM-5

Cu/Cr/HZSM-5

Zn/Cu/Cr/HZSM-5
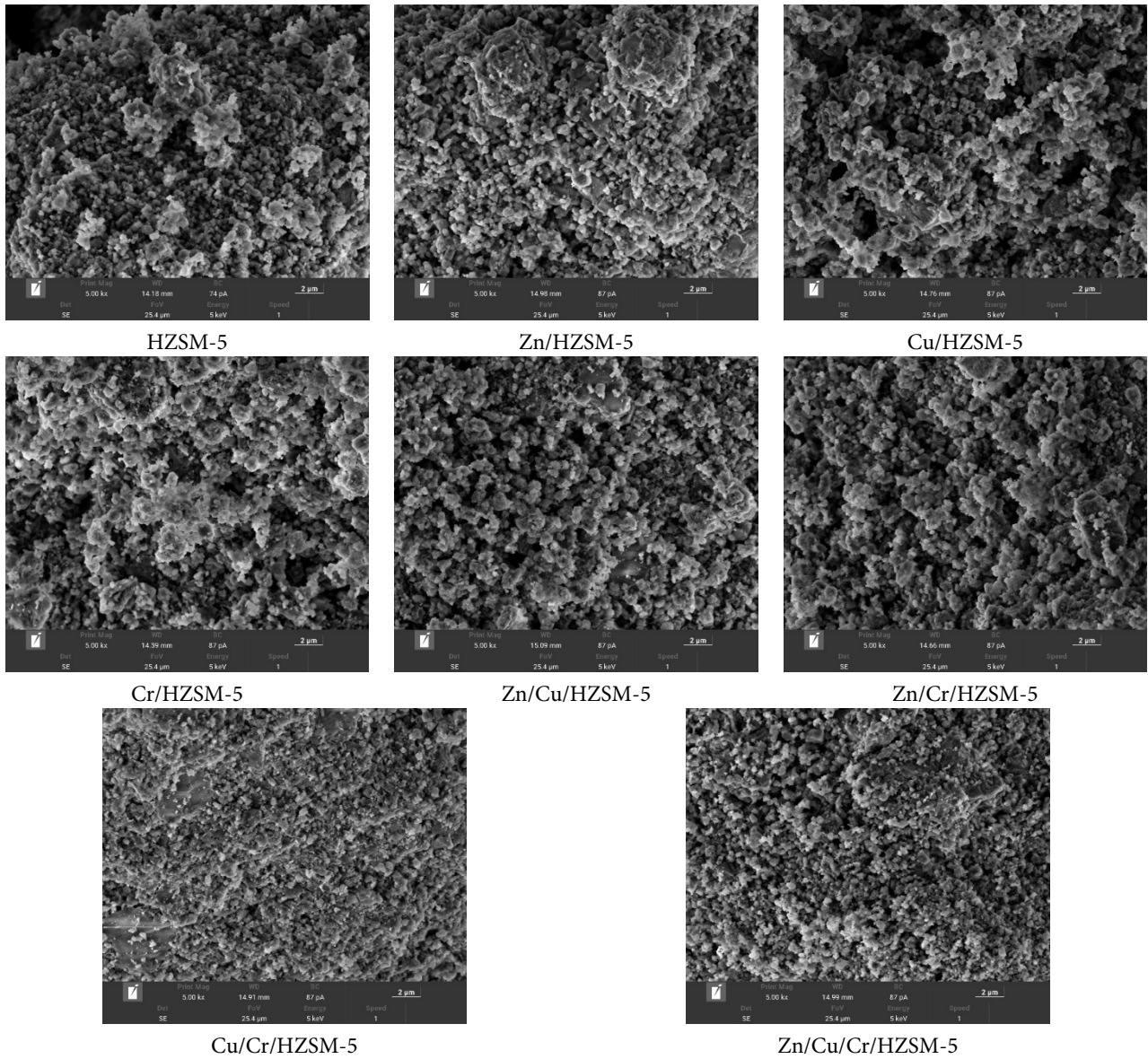
Figure 3. SEM characterization of modified HZSM-5 zeolite.
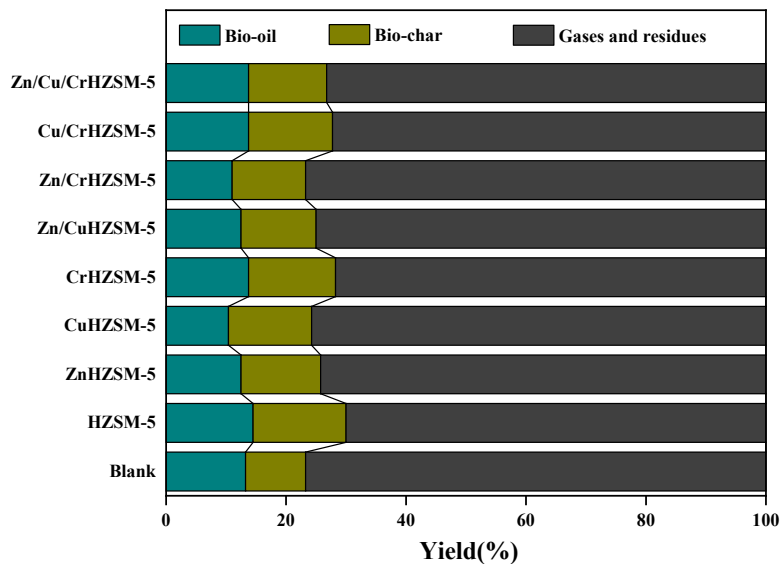
Figure 4. Effect of metal-modified HZSM-5 on HTL products of TS in urea environment.
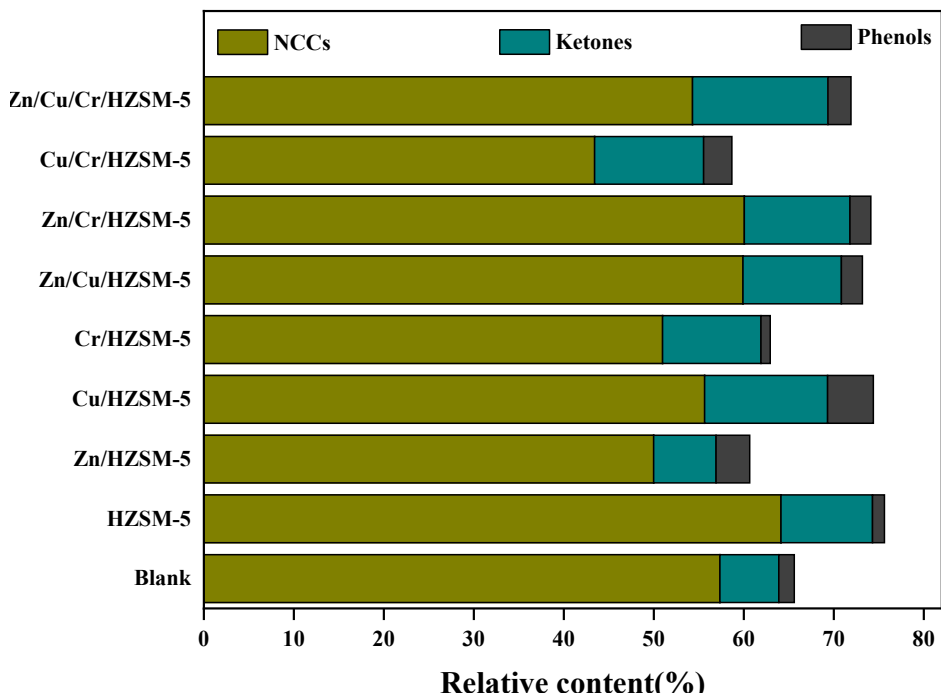
Figure 5. Effect of different metal-modified catalysts on the relative content of main chemical components in bio-oil.
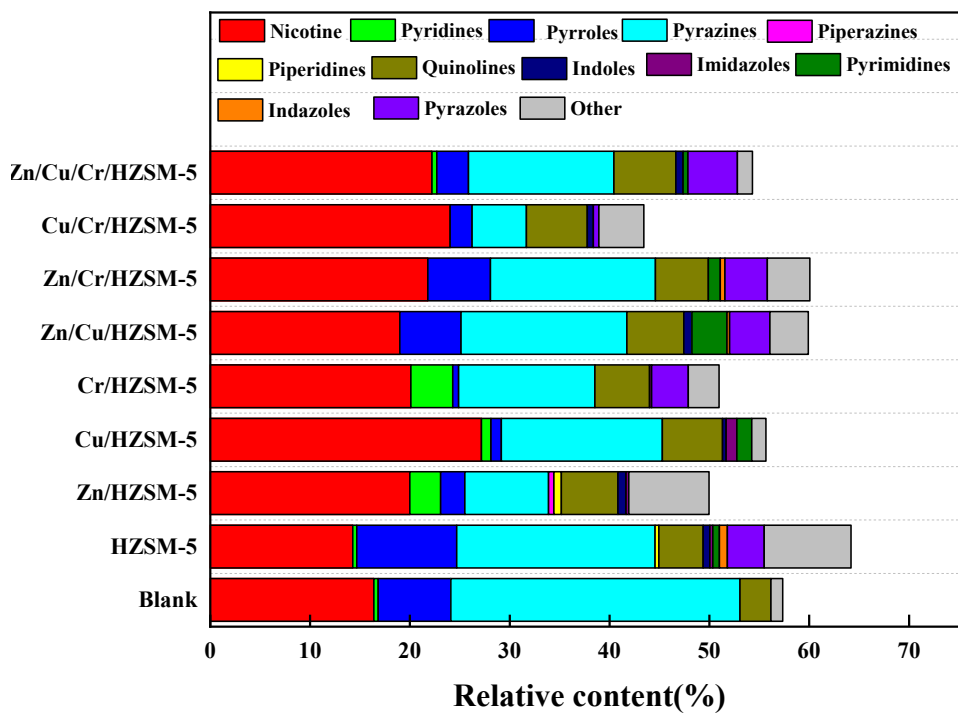
Figure 6. Effect of different metal-modified catalysts on the relative content of NCCs in bio-oil.
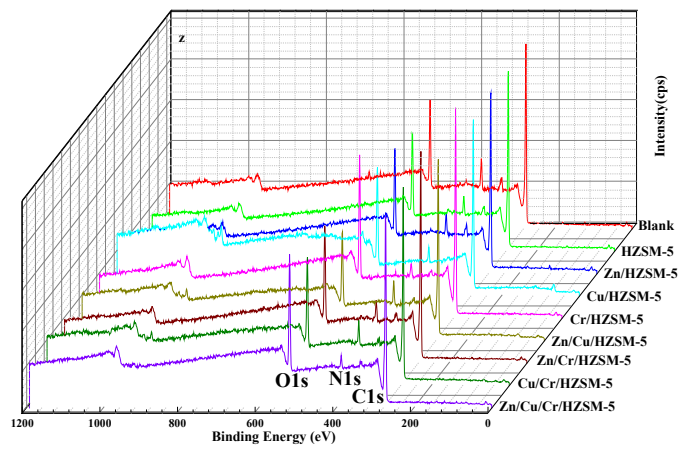
Figure 7. Total spectrum of XPS spectral analysis.
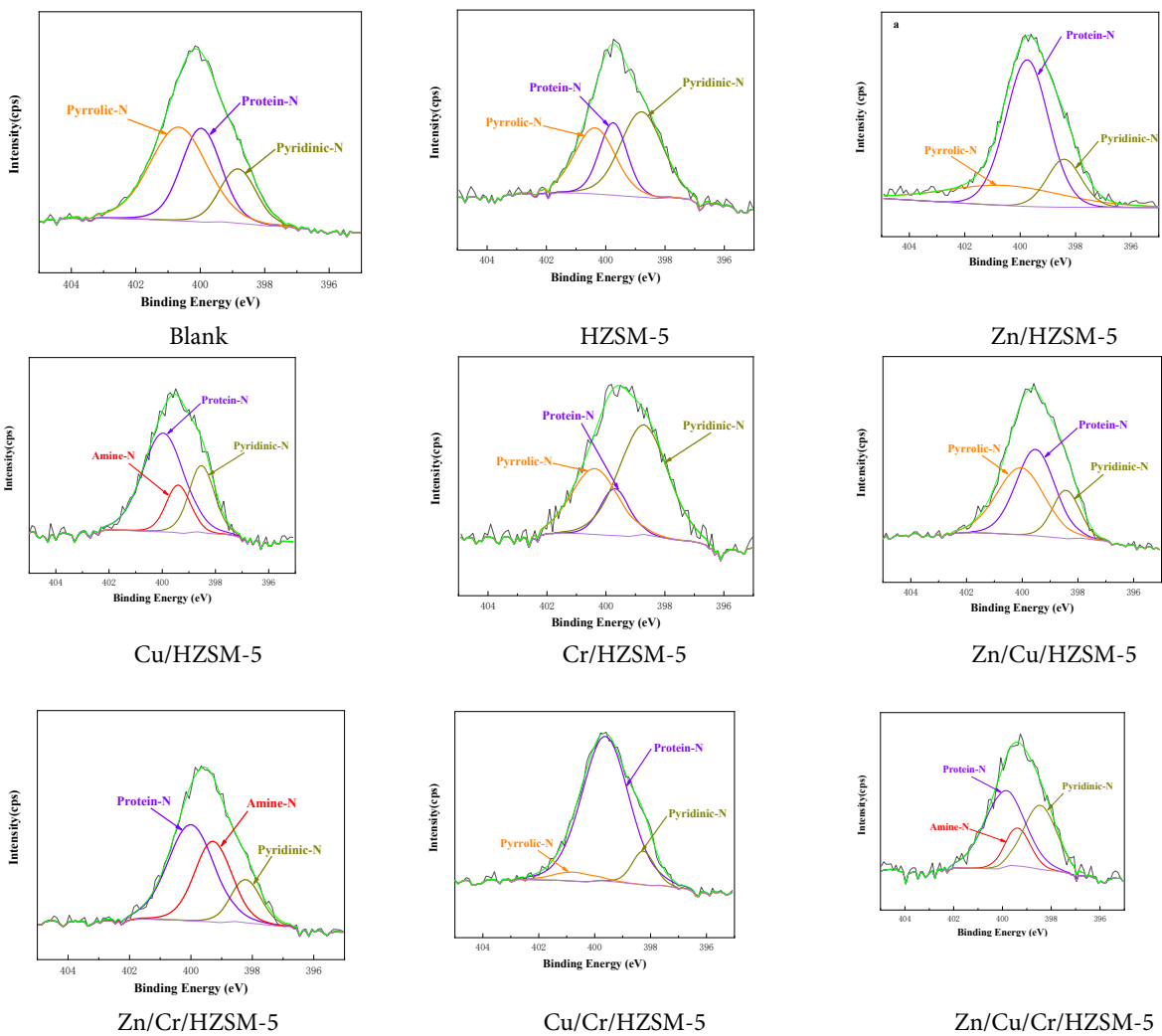
Figure 8. XPS spectra of biochar and HZSM-5-modified biochar in urea environment.

membered and six-membered cyclic NCCs, which was also the reason for the increase in the relative content of pyrrole and indole(Wu et al., 2020). However, the addition of HZSM-5 reduced the relative content of nicotine from 16.39% to 14.27%, which may be because the acidic site of HZSM-5 led to the partial decomposition of nicotine. The HZSM-5 zeolite modified by a single metal Zn, Cu, and Cr had an inhibitory effect on the relative content of NCCs. However, the three metals all promoted the generation of nicotine in bio-oil. Under the action of Zn/HZSM-5, Cu/HZSM-5, and Cr/HZSM-5, the relative contents of nicotine were 20%, 27.17%, and 20.09%, respectively. The three metals had certain selectivity for nicotine, and the copper metal had the strongest selectivity for nicotine. After HZSM-5 was modified by the three metals, the relative content of pyridine increased, whereas the relative content of pyrrole and pyrazine decreased. With the modification of Cr metal, the relative content of pyridine increased to 4.19%. Cr/HZSM-5 had the strongest selectivity for pyridine. The influence of bimetallic-modified HZSM-5 on the relative content of NCCs was as follows: the relative content of NCCs was 59.9% under Zn/Cu/HZSM-5 catalytic liquefaction, 60.06% under Zn/Cr/HZSM-5 catalytic liquefaction, and 43.42% under Cu/Cr/HZSM-5 catalytic liquefaction. Thus, the content of NCCs after the interaction of Zn, Cu and Zn, Cr was more than that after the modification of a single metal. However, after the joint modification of Cu and Cr, the inhibition effect on NCCs was the most serious, which was not conducive to the production of NCCs. In addition, after bimetal modification of the HZSM-5 zeolite, the relative content of nicotine was still higher than that before HZSM-5 zeolite addition. The Cu/Cr/HZSM-5 zeolite was more selective to nicotine but not as selective as single metal Zn/HZSM-5. The tri metal-modified HZSM-5 zeolite had no obvious selectivity advantage for NCCs. The total relative content of NCCs decreased, the relative content of nicotine still increased, and the relative content of pyrazine dropped. Summing up all nine experiments, whether the HZSM-5 zeolite catalyzes or not, the relative content of nicotine was inversely related to the relative content of pyrazine. The increase in the relative content of nicotine was accompanied with the decrease in the relative content of pyrazine, which fully proved a conversion relationship between nicotine and pyrazine (Baker & Bishop, 2005; Cardoso & Ataide, 2013; Xia et al., 2021).

3.4. Effect of catalysts on bio-char distributions

To further discuss the mechanism related to HTL of TS under urea environment and understand the migration of N in biochar after HZSM-5 zeolite modification, we conducted XPS spectral analysis on biochar samples, as shown in Figure 7 and 8.

Figure 7 shows that all samples were composed of three different peaks: C1s, N1s, and O1s, and their binding energies were 282, 397, and 529 eV, respectively (Zheng et al., 2020). Without HZSM-5, the total peak that N1s accounted for was 6.82%; after adding zeolite,

HZSM-5 accounted for 4.13%, Zn/HZSM-5 accounted for 5.21%, Cu/HZSM-5 accounted for 3.56%, Cr/HZSM-5 accounted for 3.08%, Zn/Cu/HZSM-5 accounted for 5.38%, Zn/Cr/HZSM-5 accounted for 5.15%, Cu/Cr/HZSM-5 accounted for 5.14%, and Zn/Cu/Cr/HZSM-5 accounted for 2.41%. Thus, the addition of the HZSM-5 zeolite could decrease the total nitrogen content in biochar, which may be because some nitrogen elements entered the oil and water phases. As far as single metal-modified HZSM-5 is concerned, the content of N in biochar under Zn/HZSM-5 catalytic condition was more than that of Cu/HZSM-5 and Cr/HZSM-5, which corresponded to the relatively low content of NCCs in bio-oil under Zn/HZSM-5 catalytic condition. Under the catalysis of bimetallic-modified HZSM-5 zeolite, the content of N in the biochar was not remarkably different, and the relative contents of NCCs in the bio-oil catalyzed via the Zn/Cu/HZSM-5 zeolite and Zn/Cr/HZSM-5 zeolite did not also differ significantly. These two catalysts rarely let NCCs escape into the water phase. However, under the catalysis of Cu/Cr/HZSM-5, the relative content of NCCs in the bio-oil was low, possibly because Cu and some NCCs in the reaction products were lost to the aqueous phase due to the interaction of Cr metal. For Zn/Cu/Cr/HZSM-5 modified by the three metals, the proportion of N content was the least, and the NCCs in the bio-oil did not improve significantly, so a large amount of N was also lost to the water phase(Garcia Alba et al., 2013).

The nitrogen source in this experiment mainly resulted from the protein-N in TS itself and inorganic N brought by adding urea (Yu et al., 2011). As shown in Fig. 8, after HTL in 2% urea solution, XPS spectral analysis of its biochar displayed that the N compounds in the biochar were mainly composed of pyridinic-N (398.5 ± 0.3 eV), ammonia-N (399.4 ± 0.1 eV), protein-N (399.8 ± 0.3 eV), and pyrrolic-N (400.5 ± 0.3 eV)(Chen et al., 2017; Dai et al., 2017; F. Huang et al., 2018). Without the HZSM-5 catalyst, the main nitrogen components in the biochar after the reaction were pyridinic-N, protein-N, and pyrrolic-N, with pyrrolic-N accounting for 48.39% of the total. After adding HZSM-5, the protein-N content in the biochar increased except for Cr/HZSM-5. Protein-N in the biochar generated by the Cr/HZSM-5 catalyst accounted for 13.79, with a serious decrease in the relative content. The addition of Cr/HZSM-5 promoted the self-condensation or Maillard reaction of amino acids, or Cr/HZSM-5 promoted the conversion of pyridinic-N and pyrrolic-N in biochar to pyridine in bio-oil, which verified the sharp increase in the relative content of pyridine in bio-oil after the catalytic reaction of Cr/HZSM-5. After the Cu/Cr/HZSM-5 reaction, the protein-N content in the biochar was the largest at 85.81%. A large amount of protein in TS had not been completely decomposed. This abnormal situation may be caused by the malignant competition of Cu and Cr for acid sites, which was also mutually verified by the relatively small content of NCCs in bio-oil after the Cu/Cr/HZSM-5 catalytic reaction.
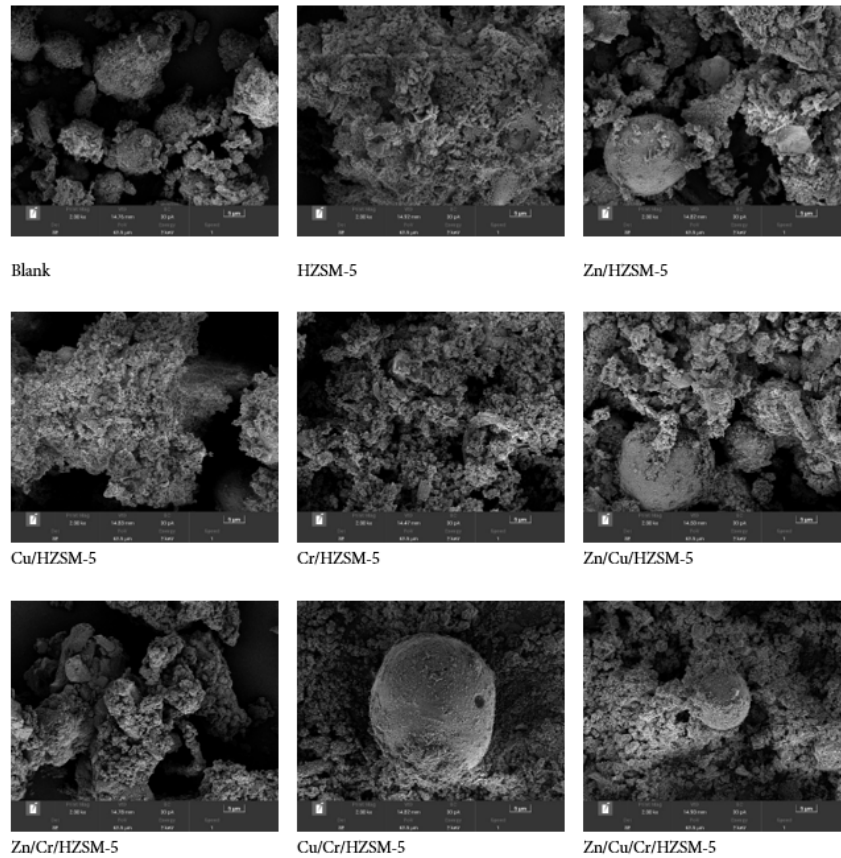
Figure 9. SEM of biochar after catalytic liquefaction of modified HZSM-5 in urea environment.
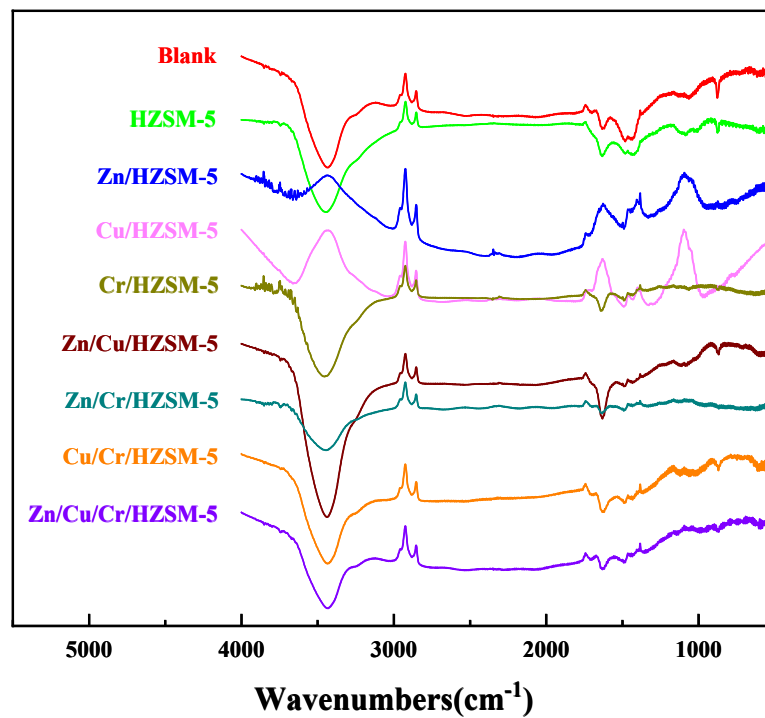
Figure 10. FT-IR of biochar after catalytic liquefaction of modified HZSM-5 in urea environment.
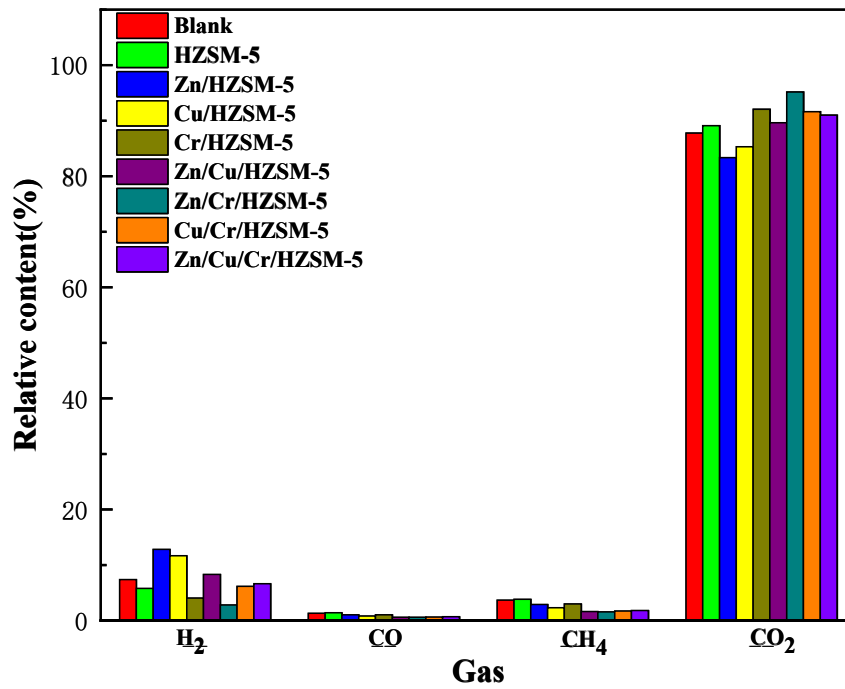
Figure 11. Effect of metal-modified HZSM-5 zeolite on gas generation
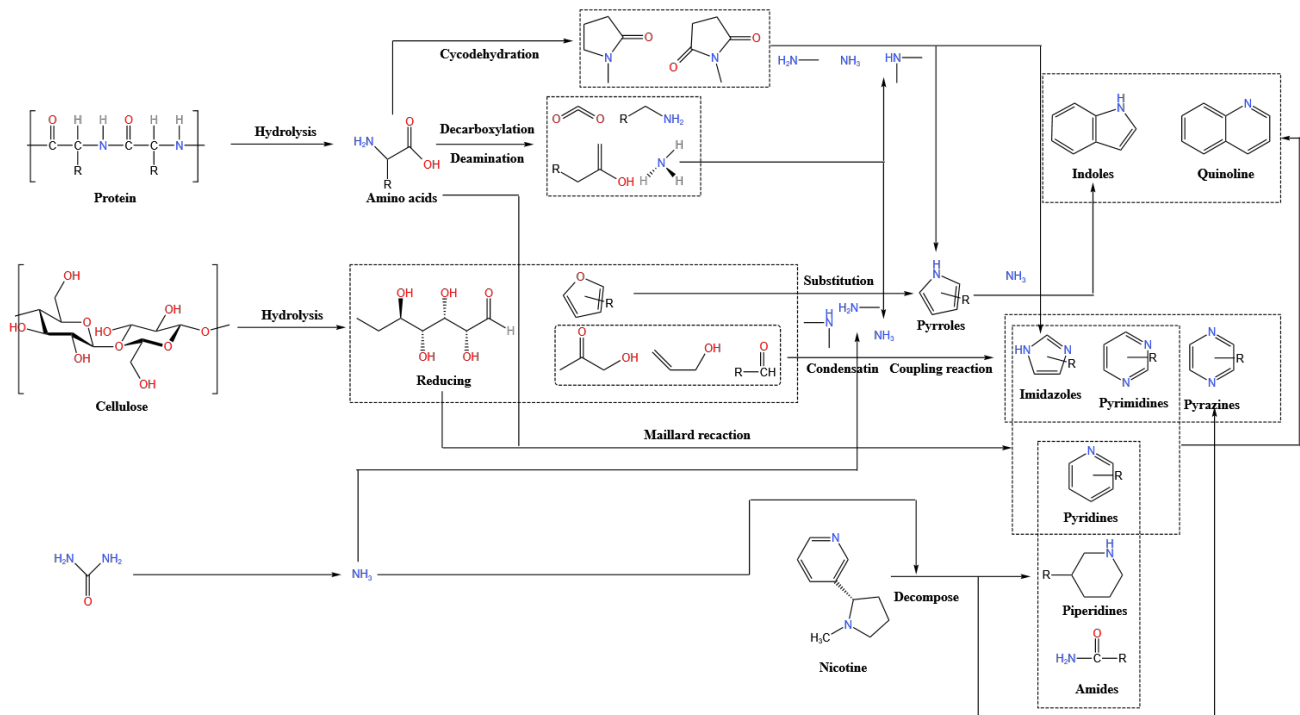
Figure 12. Possible reaction pathways of TS with urea and HZSM-5 to produce NCCs

SEM morphology analysis of biochar is convenient for us to understand the overall situation of biochar generated after the TS reaction. Fig. 9 shows the SEM images of biochar after HTL. The SEM image of biochar shows that the overall shape of biochar under the HZSM-5 catalytic conditions was dense, with few large particles. The biochar after Cu/Cr/HZSM-5 catalytic liquefaction revealed aggregates of super large particles. The SEM images of biochar under the catalytic liquefaction of the Zn/HZSM-5 zeolite and Zn/Cu/HZSM-5 zeolite were similar, which also proved that Zn metal was dominant under the co-modification of Zn and Cu.

Figure 10 displays the FT-IR of nine different types of biochar. Figure 10 shows that the influence of Zn/HZSM-5 and Cu/HZSM-5 on biochar was relatively obvious compared with that of other modified catalysts. The tensile vibration peaks of O-H bond and N-H bond between 3000 and 3650 cm^{-1} were attributed to the presence of water content, carboxylic acid, amide, and other substances (Wei et al., 2023). The weak peak strength between 3000 and 3650 cm^{-1} under the catalytic conditions of the Zn/HZSM-5 and Cu/HZSM-5 zeolites was mainly due to the relatively few O-H bonds in the biochar, most of which entered the oil phase to form phenols. The relatively high content of phenols in the oil phase analyzed via GC-MS corresponded to the few O-H bonds in biochar. The strong absorption peak at 2952–2872 cm^{-1} represented symmetric and asymmetric C – H bond tensile vibrations, indicating the presence of alkyl C – H(Fan, Hornung, Dahmen, & Kruse, 2018). The characteristic absorption peaks of benzene ring in lignin appeared at 1607, 1510, 1462, and 834 cm^{-1} (Long et al., 2016).

3.5. Effect of catalysts on the gas phase

After HTL, the gas products generated were determined by GC. Figure 11 shows that the main gases produced were CO_2, H_2, and CH_4; the relative content of CO was basically 0, which could be ignored. Among all the modified catalysts, Zn/HZSM-5 had the best selectivity for hydrogen, and the relative content of H_2 was 12.78%. The production of H_2 is related to the decomposition of ammonia at high temperatures. Hydrogen ions generated by ammonia decomposition and hydrogen ions generate hydrogen from each other. However, the relatively high content of H_2 in Zn/HZSM-5 may be due to the fact that the hydrolysis of Zn could also produce a certain amount of H_2 (Cheng et al., 2017). The relative content of CO_2 under each catalyst accounted for more than 80%, which showed that a large number of decarboxylation reactions occurred in the HTL process (Balat, 2008). The relatively low content of CH_4 was generally due to the decomposition of methoxy (Brand et al., 2013).

3.6 Possible reaction mechanism of NCC formation

On the basis of the analysis of the above results and the reaction mechanism summarized by our predecessors, the possible reaction mechanism in this experiment is summarized in Figure 12.

The possible reaction mechanism for the formation of various NCCs in the HTL of TS by adding urea and HZSM-5 mainly involved the decomposition process of protein, cellulose, and nicotine. NH_3 from urea decomposition can generate NH^* and NH_2^* under the action of TS, as shown in Equation (4) (Chen et al., 2016). Protein is first decomposed into amino acids, and some of the amino acids will react with the reducing sugar generated from cellulose hydrolysis to generate imidazole, pyrimidine, and pyridine. Some of them are self-condensed to form cyclic imines, and the cyclic imines generate pyrrole and imidazole under the action of NH^*, NH_2^*, and NH_3. Another part of amino acids generates carbon dioxide and amine through decarboxylation, and organic acid and ammonia are generated through deamination. The formation of amine and ammonia introduces NH^*, NH_2^*, and NH_3 into the hydrothermal reaction, and these ions participate in each reaction stage of HTL, creating conditions for the formation of NCCs. In HTL, cellulose will hydrolyze to form reducing sugar, which will react with amino acids in the Maillard reaction. In addition, cellulose can be hydrolyzed to produce furan and light oxygenated chemicals. Furan can generate pyrrole chemicals under the replacement of ammonium ions provided by urea and amino acids, whereas pyrrole may generate indole under the action of ammonium ions. The oxygenated chemicals generated from cellulose hydrolysis can react with ammonium ions to generate imidazole, pyrimidine, and pyrazine. The main products of nicotine decomposition are pyridine, piperidine, amide, and pyrazine:

$$C_{biomass} + NH_3 \rightarrow C^* + H^* + NH^* + NH_2^* \qquad (4)$$
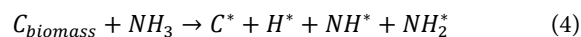
4. Conclusion

This experiment studied the effect of Zn, Cu, and Cr metal-modified HZSM-5 on the NCCs in the HTL products of TS in an urea environment. HZSM-5 could promote the preparation of NCCs from TS by HTL, and the relative content of NCCs reached 64.13% after HTL. After the HZSM-5 zeolite was modified with Zn, Cu, Cr, and other metals (whether single metal, bimetallic, or tri metal), obvious selectivity to nicotine was observed. The relative content of nicotine reached 27.17% under the catalysis of the Cu/HZSM5 zeolite. Cr/HZSM-5 had the most obvious selectivity for pyrrole. The addition of Cr/HZSM-5 increased the content of pyrrole to 4.19%. Compared with HZSM-5, the coking rate of HZSM-5 modified by Zn, Cu, and Cr was lower, and Zn/HZSM-5 benefitted the increase in the N content in biochar in the reaction products.

Author contributions

JB contributed to conceptualization, experimentation, original draft writing, review and editing, supervision, and funding acquisition. LL and HL were involved in experimentation, data analysis, and

draft preparation. PL and CC contributed to data analysis, graph preparation, and review and editing.

Acknowledgment
The authors were grateful to their department.

Competing financial interests
The authors have no conflict of interest.

Competing Financial Interests
Authors declare that there are no financial or non-financial interests that are directly or indirectly related to the work. No patent is under evaluation related to this work.

Ethics approval
Not applicable

References

Baker, R. R., & Bishop, L. J. (2005). The pyrolysis of non-volatile tobacco ingredients using a system that simulates cigarette combustion conditions. Journal of Analytical and Applied Pyrolysis, 74(1-2), 145-170. doi:10.1016/j.jaap.2004.10.011

Balat, M. (2008). Mechanisms of thermochemical biomass conversion processes. Part 3: Reactions of liquefaction. Energy Sources Part a-Recovery Utilization and Environmental Effects, 30(7), 649-659. doi:10.1080/10407780600817592

Banozic, M., Babic, J., & Jokic, S. (2020). Recent advances in extraction of bioactive compounds from tobacco industrial waste-a review. Industrial Crops and Products, 144, 112009. doi:10.1016/j.indcrop.2019.112009

Brand, S., Susanti, R. F., Kim, S. K., Lee, H. S., Kim, J., & Sang, B. I. (2013). Supercritical ethanol as an enhanced medium for lignocellulosic biomass liquefaction: Influence of physical process parameters. Energy, 59, 173-182. doi:10.1016/j.energy.2013.06.049

Cardoso, C. R., & Ataide, C. H. (2013). Analytical pyrolysis of tobacco residue: Effect of temperature and inorganic additives. Journal of Analytical and Applied Pyrolysis, 99, 49-57. doi:10.1016/j.jaap.2012.10.029

Chen, W., Yang, H. P., Chen, Y. Q., Chen, X., Fang, Y., & Chen, H. P. (2016). Biomass pyrolysis for nitrogen-containing liquid chemicals and nitrogen-doped carbon materials. Journal of Analytical and Applied Pyrolysis, 120, 186-193. doi:10.1016/j.jaap.2016.05.004

Chen, W., Yang, H. P., Chen, Y. Q., Xia, M. W., Chen, X., & Chen, H. P. (2017). Transformation of Nitrogen and Evolution of N-Containing Species during Algae Pyrolysis. Environmental Science & Technology, 51(11), 6570-6579. doi:10.1021/acs.est.7b00434

Cheng, S. Y., Wei, L., Alsowij, M., Corbin, F., Boakye, E., Gu, Z. R., & Raynie, D. (2017). Catalytic hydrothermal liquefaction (HTL) of biomass for bio-crude production using Ni/HZSM-5 catalysts. Aims Environmental Science, 4(3), 417-430. doi:10.3934/environsci.2017.3.417

Cheng, S. Y., Wei, L., Julson, J., Kharel, P. R., Cao, Y. H., & Gu, Z. R. (2017). Catalytic liquefaction of pine sawdust for biofuel development on bifunctional Zn/HZSM-

5 catalyst in supercritical ethanol. Journal of Analytical and Applied Pyrolysis, 126, 257-266. doi:10.1016/j.jaap.2017.06.001

Cheng, S. Y., Wei, L., & Rabnawaz, M. (2018). Catalytic liquefaction of pine sawdust and in-situ hydrogenation of biocrude over bifunctional Co-Zn/HZSM-5 catalysts. Fuel, 223, 252-260. doi:10.1016/j.fuel.2018.03.043

Dai, J. H., Zhu, L. F., Tang, D. Y., Fu, X., Tang, J. Q., Guo, X. W., & Hu, C. W. (2017). Sulfonated polyaniline as a solid organocatalyst for dehydration of fructose into 5-hydroxymethylfurfural. Green Chemistry, 19(8), 1932-1939. doi:10.1039/c6gc03604j

Fan, Y., Hornung, U., Dahmen, N., & Kruse, A. (2018). Hydrothermal liquefaction of protein-containing biomass: study of model compounds for Maillard reactions. Biomass Conversion and Biorefinery, 8(4), 909-923. doi:10.1007/s13399-018-0340-8

Feng, L. H., Li, Z. X., Hong, C., Xing, Y., Qin, Y., Lu, Y. T., . . . Lu, J. W. Characteristic analysis of bio-oil from penicillin fermentation residue by catalytic pyrolysis. Environmental Technology. doi:10.1080/09593330.2022.2034980

Gao, H., Bai, J., Wei, Y., Chen, W., Li, L., Huang, G., . . . Chang, C. (2022). Effects of drying pretreatment on microwave pyrolysis characteristics of tobacco stems. Biomass Conversion and Biorefinery. doi:10.1007/s13399-021-02120-6

Garcia Alba, L., Vos, M. P., Torri, C., Fabbri, D., Kersten, S. R., & Brilman, D. W. (2013). Recycling nutrients in algae biorefinery. ChemSusChem, 6(8), 1330-1333. doi:10.1002/cssc.201200988

Guo, G. N., Cai, B., Li, R., Pan, X., Wei, M., & Zhang, C. (2021). Enhancement of saccharification and ethanol conversion from tobacco stalks by chemical pretreatment. Biomass Conversion and Biorefinery, 11(4), 1085-1092. doi:10.1007/s13399-019-00478-2

Huang, F., Li, W. Z., Liu, Q. C., Zhang, T. W., An, S. X., Li, D. W., & Zhu, X. F. (2018). Sulfonated tobacco stem carbon as efficient catalyst for dehydration of C6 carbohydrate to 5-hydroxymethylfurfural in gamma-valerolactone/water. Fuel Processing Technology, 181, 294-303. doi:10.1016/j.fuproc.2018.09.026

Huang, Z. G., Yu, Z. S., Li, M. R., Bin, Y. H., Zhang, X. K., Wei, C., . . . Ma, X. Q. (2022). Catalytic co-pyrolysis of Chlorella vulgaris and urea: Thermal behaviors, product characteristics, and reaction pathways. Journal of Analytical and Applied Pyrolysis, 167, 105667. doi:10.1016/j.jaap.2022.105667

Kang, K., Quitain, A. T., Daimon, H., Noda, R., Goto, N., Hu, H. Y., & Fujie, K. (2001). Optimization of amino acids production from waste fish entrails by hydrolysis in sub- and supercritical water. Canadian Journal of Chemical Engineering, 79(1), 65-70. doi:10.1002/cjce.5450790110

Khanmohammadi, S., Atashkari, K., & Kouhikamali, R. (2016). Modeling and Assessment of a Biomass Gasification Integrated System for Multigeneration Purpose. International Journal of Chemical Engineering, 2639241 (2639211 pp.)-2639241 (2639211 pp.). doi:10.1155/2016/2639241

Khoshbin, R., & Haghighi, M. (2013). Direct syngas to DME as a clean fuel: The beneficial use of ultrasound for the preparation of CuO-ZnO-Al2O3/HZSM-5 nanocatalyst. Chemical Engineering Research & Design, 91(6), 1111-1122. doi:10.1016/j.cherd.2012.11.017

Li, J. Y., Tang, X. L., Yi, H. H., Yu, Q. J., Gao, F. Y., Zhang, R. C., . . . Chu, C. (2017). Effects of copper-precursors on the catalytic activity of Cu/graphene catalysts for the selective catalytic oxidation of ammonia. Applied Surface Science, 412, 37-44. doi:10.1016/j.apsusc.2017.03.227

Li, L., Bai, J., Liu, Q., Huang, G., Song, J., Chang, C., . . . Pang, S. (2022). Performance research and optimization of the production of high-value nitrogen-containing compounds from tobacco stems via two-step hydrothermal liquefaction. Biomass Conversion and Biorefinery. doi:10.1007/s13399-022-03006-x

Li, X., Wang, J., Fan, Y., Liu, S., & Cai, Y. (2017). Fe, Co and Cu Modified HZSM-5 Catalysts for Online Upgrading of Pyrolysis Vapors from Rape Straw. Transactions of the Chinese Society for Agricultural Machinery, 48(2), 305-313. Retrieved from <Go to ISI>://CSCD:5928274

Liu, H. M., Shen, W. J., Liu, X. M., Bao, X. H., & Xu, Y. (2004). Effect of acid treatment of zeolite on catalytic performance of Mo/HZSM-5 for methane dehydroaromatization. Chinese Journal of Catalysis, 25(9), 688-692. Retrieved from <Go to ISI>://WOS:000224401400004

Long, J. X., Li, Y. W., Zhang, X., Tang, L., Song, C. H., & Wang, F. R. (2016). Comparative investigation on hydrothermal and alkali catalytic liquefaction of bagasse: Process efficiency and product properties. Fuel, 186, 685-693. doi:10.1016/j.fuel.2016.09.016

Ong, H. C., Chen, W. H., Farooq, A., Gan, Y. Y., Lee, K. T., & Ashokkumar, V. (2019). Catalytic thermochemical conversion of biomass for biofuel production: A comprehensive review. Renewable & Sustainable Energy Reviews, 113, 109266. doi:10.1016/j.rser.2019.109266

Pan, Y. H., Song, J. X., Lou, F. F., Xu, J., Zhou, Y. G., & Huang, Q. X. (2022). Catalytic co-pyrolysis of rubber waste and polyacrylonitrile for producing BTEX enriched oil via heterogeneous Diels-Alder reaction. Fuel, 321, 124028. doi:10.1016/j.fuel.2022.124028

Ponnusamy, V. K., Nagappan, S., Bhosale, R. R., Lay, C. H., Nguyen, D. D., Pugazhendhi, A., . . . Kumar, G. (2020). Review on sustainable production of biochar through hydrothermal liquefaction: Physico-chemical properties and applications. Bioresource Technology, 310, 123414. doi:10.1016/j.biortech.2020.123414

Ren, Y. M., Zhang, J. M., Xu, Q., Chen, Z. M., Yang, D. Y., Wang, B., & Jiang, Z. (2014). Biomass-derived three-dimensional porous N-doped carbonaceous aerogel for efficient supercapacitor electrodes. Rsc Advances, 4(45), 23412-23419. doi:10.1039/c4ra02109f

Wang, K., Zhao, N., Lei, S. W., Yan, R., Tian, X. D., Wang, J. Z., . . . Liu, L. (2015). Promising biomass-based activated carbons derived from willow catkins for high performance supercapacitors. Electrochimica Acta, 166, 1-11. doi:10.1016/j.electacta.2015.03.048

Wei, Y. Y., Fakudze, S., Yang, S. L., Zhang, Y., Xue, T. J., Han, J. A., & Chen, J. Q. (2023). Synergistic citric acid-surfactant catalyzed hydrothermal liquefaction of pomelo peel for production of hydrocarbon-rich bio-oil. Science of the Total Environment, 857, 159235. doi:10.1016/j.scitotenv.2022.159235

Wu, H. H., Wang, L., Ji, G. B., Lei, H. W., Qu, H., Chen, J., . . . Liu, J. (2020). Renewable production of nitrogen-containing compounds and hydrocarbons from catalytic microwave-assisted pyrolysis of chlorella over metal-doped HZSM-5 catalysts. Journal of Analytical and Applied Pyrolysis, 151, 104902. doi:10.1016/j.jaap.2020.104902

Xia, Q., Yan, B. C., Wang, H. W., Xu, J., Zhang, S. P., Zhou, G. J., . . . Chen, W. B. (2021). Production of bio-oils enriched with aroma compounds from tobacco waste fast pyrolysis in a fluidized bed reactor. Biomass Conversion and Biorefinery, 11(5), 1611-1619. doi:10.1007/s13399-019-00578-z

Xu, L. J., Yao, O., Zhang, Y., & Fu, Y. (2017). Integrated Production of Aromatic Amines and N-Doped Carbon from Lignin via ex Situ Catalytic Fast Pyrolysis in the Presence of Ammonia over Zeolites. Acs Sustainable Chemistry & Engineering, 5(4), 2960-2969. doi:10.1021/acssuschemeng.6b02542

Yao, Q., Xu, L. J., Han, Z., & Zhang, Y. (2015). Production of indoles via thermo-catalytic conversion and ammonization of bio-derived furfural. Chemical Engineering Journal, 280, 74-81. doi:10.1016/j.cej.2015.05.094

Yu, G., Zhang, Y. H., Schideman, L., Funk, T., & Wang, Z. C. (2011). Distributions of carbon and nitrogen in the products from hydrothermal liquefaction of low-lipid microalgae. Energy & Environmental Science, 4(11), 4587-4595. doi:10.1039/c1ee01541a

Yuan, C., Wang, S., Qian, L. L., Barati, B., Gong, X., Abomohra, A., . . . Liu, L. (2019). Effect of cosolvent and addition of catalyst (HZSM-5) on hydrothermal liquefaction of macroalgae. International Journal of Energy Research, 43(14), 8841-8851. doi:10.1002/er.4843

Zhang, X., Yuan, Z. G., Yao, Q., Zhang, Y., & Fu, Y. (2019). Catalytic fast pyrolysis of corn cob in ammonia with Ga/HZSM-5 catalyst for selective production of acetonitrile. Bioresource Technology, 290, 121800. doi:10.1016/j.biortech.2019.121800

Zhao, X. H., Wei, L., Julson, J., Gu, Z. R., & Cao, Y. H. (2015). Catalytic cracking of inedible camelina oils to hydrocarbon fuels over bifunctional Zn/ZSM-5 catalysts. Korean Journal of Chemical Engineering, 32(8), 1528-1541. doi:10.1007/s11814-015-0028-8

Zheng, Y. W., Li, D. H., Wang, J. D., Chen, Y. F., Liu, C., Lu, Y., . . . Zheng, Z. F. (2022). Ammonia (NH3)/nitrogen (N2) torrefaction pretreatment of waste biomass for the production of renewable nitrogen-containing chemicals via catalytic ammonization pyrolysis: Evolution of fuel-N under a N2/ NH3-rich atmosphere. Journal of the Energy Institute, 102, 143-159. doi:10.1016/j.joei.2022.03.011

Zheng, Y. W., Wang, Z., Liu, C., Tao, L., Huang, Y. B., & Zheng, Z. F. (2020). Integrated production of aromatic amines, aromatic hydrocarbon and N-heterocyclic bio-char from catalytic pyrolysis of biomass impregnated with ammonia sources over Zn/HZSM-5 catalyst. Journal of the Energy Institute, 93(1), 210-223. doi:10.1016/j.joei.2019.03.007

Zhuang, X. Z., Liu, J. G., Wang, C. G., Zhang, Q., & Ma, L. L. (2022). Microwave-assisted hydrothermal liquefaction for biomass valorization: Insights into the fuel properties of biocrude and its liquefaction mechanism. Fuel, 317, 123462. doi:10.1016/j.fuel.2022.123462